

RESEARCH ARTICLE | APRIL 18 2013

Rheology as a tool to follow hybrid nanocomposites preparation

Manuel Oliveira; Ana Vera Machado



AIP Conf. Proc. 1526, 248–257 (2013)

<https://doi.org/10.1063/1.4802619>



View
Online



Export
Citation

CrossMark

Articles You May Be Interested In

Some Chemical Properties of Element 43

J. Chem. Phys. (December 2004)

Decoupling the interplay of polymer properties and particle size in stability of co-continuous blend composites

Physics of Fluids (May 2023)

Phase morphology and fracture behaviour of CNT and thermoplastic modified epoxy ternary nanocomposite by different processing methods

AIP Conference Proceedings (January 2020)

08 September 2023 08:43:09

AIP Advances

Why Publish With Us?



25 DAYS
average time
to 1st decision



740+ DOWNLOADS
average per article



INCLUSIVE
scope

[Learn More](#)

Rheology as a Tool to Follow Hybrid Nanocomposites Preparation

Manuel Oliveira and Ana Vera Machado

*IPC –Institute for Polymers and Composites/I3N, Department of Polymer Engineering,
University of Minho, 4800-058 Guimarães, Portugal*

Abstract. Hybrid nanocomposites were prepared using two polymeric matrices and the one inorganic precursor. Rheological measurements were performed in order to characterize and follow the reactions and to assess the effect of temperature and time on the nanocomposite structure. The experimental results evidenced that crosslinking occurs for both polymers. Higher crosslinking density and well dispersed nanoparticles morphology were achieved with EVA.

Keywords: Rheology, Sol-gel reactions, Hybrid polymers nanocomposites.

PACS: 81.05.Qk, 81.07.Pr, 61.25.hp, 82.33.Ln

INTRODUCTION

Polymer nanocomposites are a new class of materials with remarkable properties. In fact, a small amount of well dispersed inorganic filler can improve significantly the properties of a conventional polymer, such as, gas permeability, thermal stability, flame retardance, mechanical performance or chemical resistance [1-3].

Even though a lot of research has been performed on the preparation of these materials [4-6], the homogeneous dispersion of nanoparticles in polymeric matrices, especially in non-polar, is still difficult. Thus, frequently nanocomposites exhibit worst properties than conventional polymers, which limit their successful application [7-9]. Three main approaches have been used to disperse nanoparticles in a polymeric matrix: solution dispersion, melting mixing and in situ nanoparticles formation by a sol-gel process. The last, based on a reaction between a precursor, containing the inorganic particle, and a polymer allow to obtain nanoparticles homogeneously dispersed and is compatible with current industrial process, like extrusion.

Therefore, the present study aims to follow the chemical reaction (crosslinking/branching) and morphology development during the preparation of polypropylene (PP) and ethylene vinyl acetate (EVA) nanocomposites. The effect of temperature and reaction time on the nanocomposite structure was investigated. These materials, containing aluminium, were produced by sol-gel reactions by melt mixing. Rheological measurements were used to characterize the structure of the developed nanocomposites.

EXPERIMENTAL

Materials

Polypropylene modified with maleic anhydride (PP-g-MA, Polybond 3200) with a melting temperature around 160°C and a maleic anhydride content of 1 wt.%, was supplied by Crompton. Ethylene-vinyl acetate (EVA) with 12 wt.% (EVA12, Escorene Ultra UL 00112, melting temperature of 96°C) and 27 wt.% (EVA27, Escorene Ultra UL 00328, melting temperature of 71°C) of vinyl acetate, were supplied by Exxon Mobil. Aluminium isopropoxide (Al(Pr-i-O)₃), used as received in powder state, was supplied by Sigma Aldrich.

Processing

For both systems, the polymer and aluminium alkoxide concentrations were defined as 75/25 (w/w). The nanocomposites were produced by melt mixing, in a Haake batch mixer (Rheocord 90; volume 60 cm³), equipped with two rotors running in a counter-rotating way. The rotor speed was 50 rpm and the set temperature was 90°C for EVA and 180°C (200 and 220°C) for PP-g-MA nanocomposites, respectively. The following procedure was implemented to produce the materials, first pellets of the polymers were introduced into the hot mixer, after 3 min the aluminium precursor was added. The sol-gel reaction proceeded during 10 min and the total sample was removed. The hybrid polymer nanocomposite (HPN) synthesized with PP-g-MA was called HPNPP, with EVA12 was HPNEVA12 and the one with EVA27 was HPNEVA27.

Materials Characterization

Oscillatory rheological measurements were carried out using a PaarPhysica MCR300 rheometer at 180 and 90°C for HPNPP and HPNEVA, respectively. The gap and diameter of the plates was 1 mm and 25 mm, respectively. Nitrogen atmosphere was used to prevent thermo-oxidative degradation. A frequency sweep from 0.01 to 100 Hz under constant strain in the linear viscoelastic region was performed for each sample.

Infrared spectra (FT-IR) measurements were recorded in transmission mode between 400 and 4000 cm⁻¹ using a Perkin Elmer 1610, with 32 scans and resolution of 4 cm⁻¹. Thin films were previously prepared by compression moulding in a hot press and analysed directly using a solid film support.

The crosslinking density was assessed from the volume swelling degree determinate at equilibrium. Around 300 mg of samples were placed in hot xylene at 140°C during 30 hours until swelling equilibrium was reached. Then, the polymer volume fraction at swelling equilibrium, v_r , was calculated as follows:

$$v_r = \frac{1}{1 + \left(\frac{m_1}{m_2}\right) \cdot \left(\frac{\rho_2}{\rho_1}\right)} \quad (1)$$

where m_1 and m_2 are, respectively, the weight of swelled sample and the weight of dried sample and ρ_1 and ρ_2 are, respectively, the polymer and solvent densities (g.cm^{-3}).

The Flory-Rehner model was used to determine the crosslinking density. This model coupled with the phantom network assumption gives a correlation between the swelling results and the number of elastic strands, ν :

$$\nu = - \left[\frac{\ln(1 - \nu_r) + \nu_r + \chi \nu_r^2}{V \left(\nu_r^{\frac{1}{3}} - 0.5 \nu_r \right)} \right] \quad (2)$$

where χ is the polymer/solvent interaction parameter, V the molar volume of solvent and ν_r is the polymer volume fraction at swelling equilibrium. The polymer/solvent interaction parameter χ was calculated as followed:

$$\chi = \frac{V(\delta_1 - \delta_2)^2}{RT + 0.34} \quad (3)$$

where δ_1 and δ_2 are the solubility parameters of polymer and solvent, respectively, V is the molar volume; R is the universal gas constant and T is the absolute temperature.

The activation energy (E_a) of the HPNPP and HPNEVA27 hybrids was determined using gel content values. The nanocomposite was prepared at three different temperatures (180, 200 and 220°C for HPNPP and 90, 100 and 110°C for HPNEVA27, respectively) according to the procedure described above and samples were collected after 3, 7 and 10 min of mixing. For all samples, the gel content was measured according to the method described in Oliveira et al. [10]. For each temperature, the crosslinking rate was determined as the slope of gel content vs. time reaction, as described by Shieh [11]. Then, the E_a was calculated from the plot of the crosslinking reaction rate at the three different temperatures as a function of the reciprocal absolute temperature, according to the Arrhenius equation:

$$\ln(k) = \ln A - \frac{E_a}{R} \frac{1}{T} \quad (4)$$

where k is the crosslinking rate, E_a is the activation energy, R is the gas constant and T is the absolute temperature.

RESULTS AND DISCUSSION

Influence of Temperature on the Structure

The rheological behaviour of the PP-based nanocomposites prepared at different temperatures was determined to assess the effect of temperature on its molecular structure. The results presented in Figure 1 show a significant difference between the viscoelastic behaviour of PP-g-MA and HPNPP. A strong increase in complex viscosity and storage modulus can be observed for all HPNPPs, but the rheological behaviour among them is similar. This increase in viscosity and storage modulus can not only be explained by the presence of inorganic filler in the PP-g-MA matrix or physical interaction but also by the formation of a branched/crosslinking structure. This is corroborated by FT-IR results presented in Figure 2. A comparison of these two spectra evidences the strong reduction of the peak intensity at 1785 cm^{-1} upon reaction with the precursor, which implies that almost all anhydride groups have reacted.

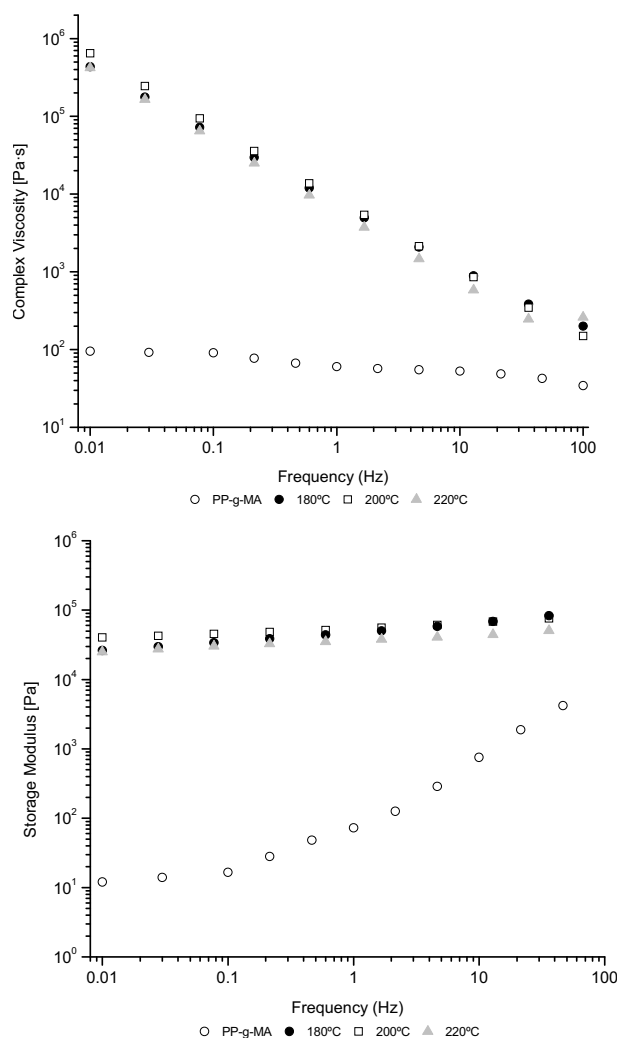


FIGURE 1. Influence of processing temperature on rheological behaviour of HPNPP.

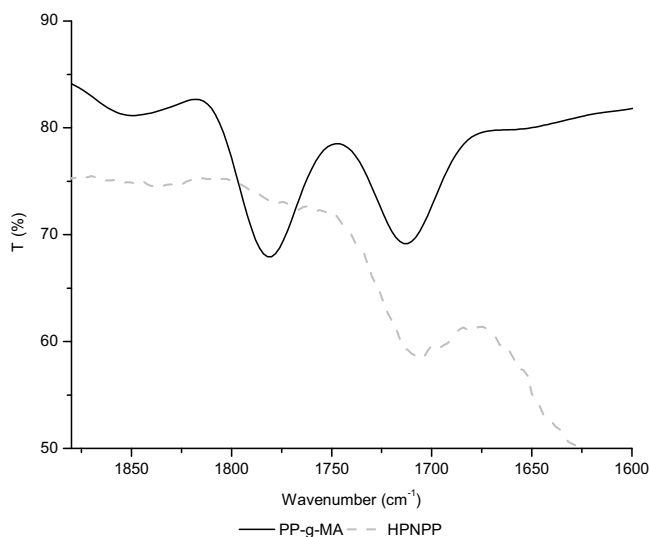


FIGURE 2. FT-IR of maleic anhydride of PP-g-MA and HPNPP.

Moreover, this rheological change can be associated with a transition from a liquid-like to a solid-like behaviour, where the storage modulus is independent of the frequency value. This type of behaviour is characteristic of the branching/crosslinking materials, which do not show a plateau at low frequencies in complex viscosity and have in the limit a slope of -1 (solid materials) [12]. The slope of the complex viscosity of the nanocomposites prepared at different temperatures is around -0.87, indicating a branching/crosslinking structure. The values of the gel content obtained for these samples were similar, which is in agreement with rheological data.

A power-law relationship (Eq. 5) can be used to analyse qualitatively the effect of the temperature on the crosslinking degree:

$$n^* = p|w|^{a-1} \quad (5)$$

where n^* is the complex viscosity, w the angular frequency and p and the a fitting parameters. The parameter $a-1$ corresponds to the slope of the curve $\log(n^*)$ vs $\log(w)$, which reflects the shear thinning behaviour. Decrease on a value represents an increase of crosslinking. The a values obtained applying Eq. 5 to complex viscosity data at 180, 200 and 220°C, are 0.087, 0.141 and 0.154, respectively. Even though the values are quite similar, it seems that at temperatures above 200°C, thermal degradation occurs.

The storage modulus of the nanocomposites appears to be constant over a broad range of frequencies. Therefore, from the theory of the rubber elasticity, the equilibrium shear elasticity modulus (G_e) can be determined based on the slope of the tangent curve to G' at low frequencies [12,13]. Using G_e and the Flory-Rehner model coupled with the phantom network it is possible to predict the crosslinking density of an imperfect network:

$$\nu = \frac{G_e}{RT} \quad (6)$$

where ν is the crosslinking density, R is the universal gas constant and T is the absolute temperature. G_e was obtained as the asymptotic value of G' at low frequency.

Applying Eq. 6 to G' data the following crosslinking density values, $7.52 \cdot 10^{-6}$, $4.58 \cdot 10^{-6}$ and $3.95 \cdot 10^{-6}$ mol.mL⁻¹, were obtained for samples prepared at 180, 200 and 220°C, respectively.

Evolution of the Chemical Reaction along the Time

The torque evolution along mixing time of HPNEVA12 and HPNEVA27 is shown in Figure 3. The first peak is associated to EVA melting followed by the addition of the aluminium precursor. For both EVAs after the addition of the precursor the torque increases, which is due to the reaction between vinyl acetate groups and aluminium precursor. Since EVA27 has more vinyl acetate groups, a more extensive reaction would be anticipated and consequently higher torque was expected. However, EVA27 (71°C) has lower melting temperature than EVA12 (96°C), which results in a decrease of viscosity and consequently lower torque for HPNEVA27. Thus, the nanocomposite torque value was always under HPNEVA12. At around 10 minutes different torque behaviour can be observed for both materials. While the torque of HPNEVA12 increases, the torque of HPNEVA27 decreases. This can be associated to network degradation decrease, as shown by Antunes et al. [14], this phenomenon occurs for materials with very high crosslinking contents.

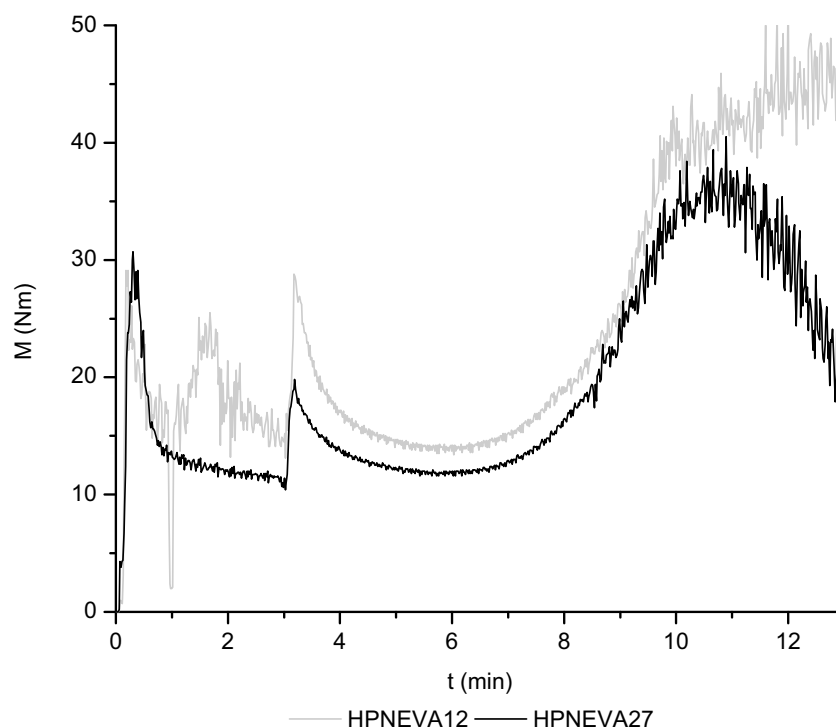


FIGURE 3. Torque evolution during HPNEVA12 and HPNEVA27 preparation.

Figure 4 shows the evolution of the storage modulus and complex viscosity along the reaction time for both HPNEVAs. An increase can be detected along the reaction time, which indicates that the reaction progresses along the time, in agreement with the torque measurements. Therefore, as the reaction takes place the material changes from liquid-like to solid-like material, where the storage modulus is independent of the frequency value. The nanocomposites prepared do not show a plateau at low frequencies and the complex viscosity has, in the limit, a slope of minus one [12].

Based on the curves slope values at 10 minutes (-0.829 and -0.885 for HPNEVA12 and HPNEVA27, respectively), the evolution of the crosslinking structure is clear. Moreover, it is possible to confirm that HPNEVA27 has higher crosslinking degree.

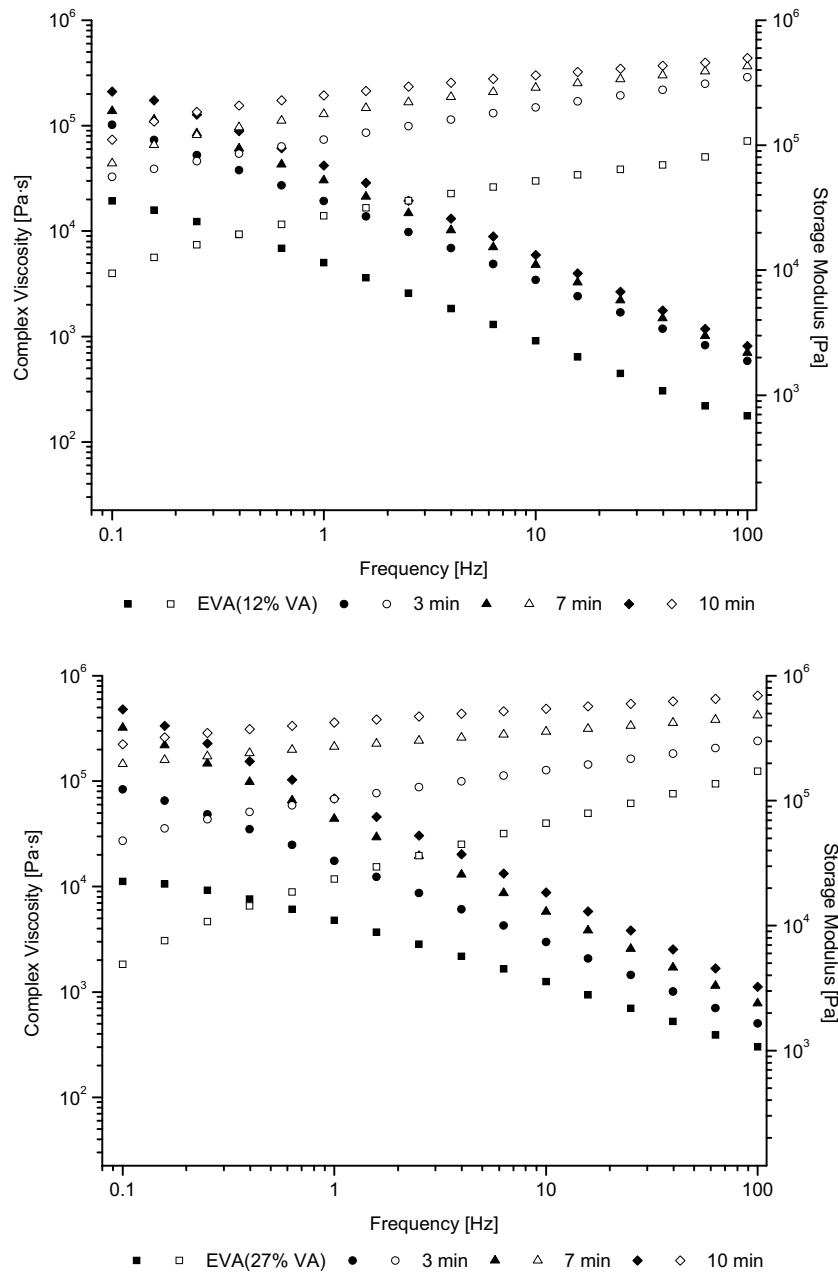


FIGURE 4. Rheological behaviour of HPNEVAs along the time.

The theoretical values of ν determined using Eq. 6 and the experimental data measured by the swelling degree experiments are presented in Figure 5.

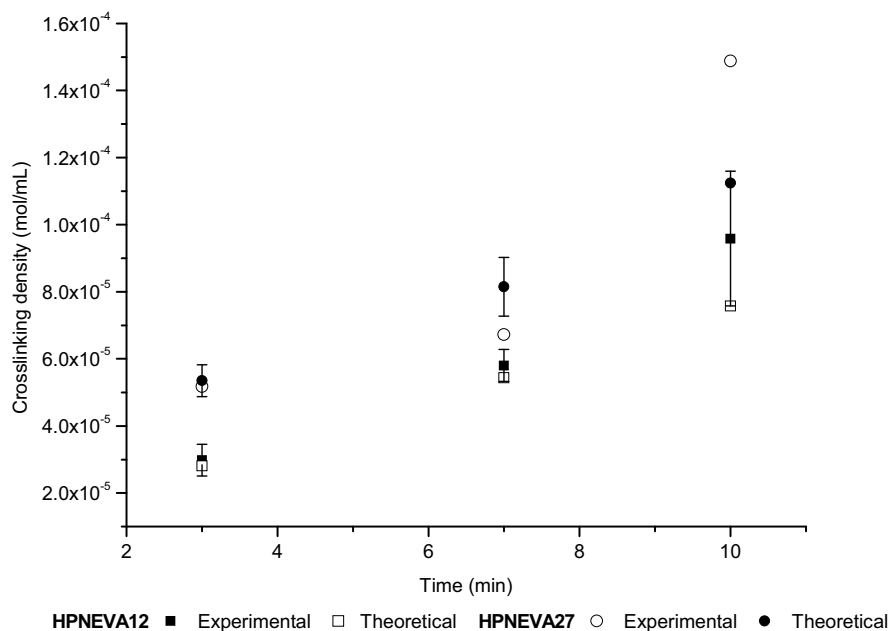


FIGURE 5. Crosslinking density evolution along the reaction time for HPNEVAs.

Both EVAs show the same trend, the crosslinking density increases along the time as a result of the reaction that is taking place. As anticipated, HPNEVA27, due to higher amount of vinyl acetate groups, reacts more to form covalent bounds with aluminium precursor and exhibits higher crosslinking density. The theoretical crosslinking density values determined are in good agreement with the swelling experimental results for reaction times of 3 and 7 min. A slightly different between theoretical and experimental values was observed for 10 min of reaction. This can be explained by the fact that at 10 min the G' values remained almost constant in a very broad range of frequencies, in this case the G_e corresponds to the constant value of G' [13].

Since a huge difference of the crosslinking density values was detected for both polymer system used, the activation energy (E_a) was determined for each polymer. The Arrhenius plots obtained for both nanocomposites are depict in Figure 6. A linear relationship was found for both, corresponding to an E_a of 52.9 kJ.mol⁻¹ and 36.3 kJ.mol⁻¹ for HPNPP and HPNEVA27, respectively. The EVA revealed to be more reactive than PP-g-MA, which can de explained by the higer amount of vinyl acetate, moreover vinyl group has a lower stereochemical hindrance when compared with maleic anhydride.

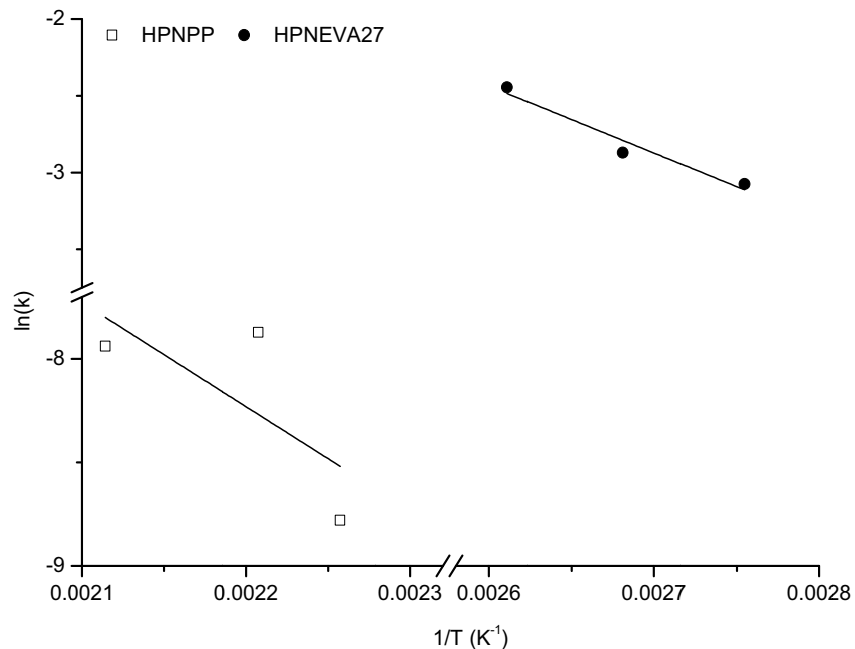


FIGURE 6. Arrhenius plots for the synthesis reactions of HPNPP and HPNEVA27.

The HPNPP and HPNEVA27 morphologies were assessed by TEM and the results are presented in Figure 7. The morphology of both HPN evidences homogeneous nanoparticles dispersed in a polymer matrix. However, due to the higher reaction extension, HPNEVA27 has smaller nanoparticles (120 nm) than HPNPP (200 nm).

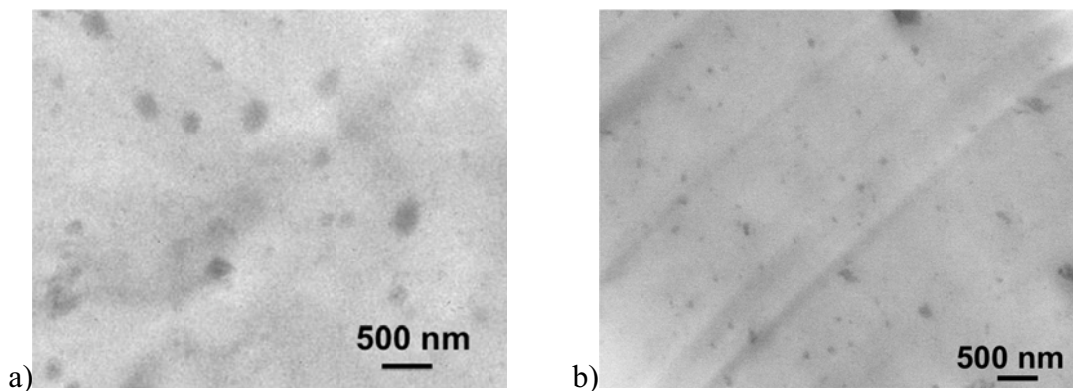


FIGURE 7. STEM pictures a) HPNPP and b) HPNEVA.

CONCLUSIONS

HPNPP present an increase on complex viscosity change from a liquid-like behaviour to a solid-like behaviour where the storage modulus is independent of the frequency. The rheological measurements showed that HPNPP had a branched/crosslinking structure and that by the preparation temperature did not have a significant influence.

The rheological measurements demonstrate that for HPNEVAs nanocomposites, the crosslinking density increases along the reaction time and HPNEVA27 reached a higher level of crosslink.

ACKNOWLEDGMENTS

The authors acknowledge the Foundation for Science and Technology (FCT) Project SFRH/BD/39085/2007 for the financial support.

REFERENCES

1. C. Sanchez, K. Shea and S. Kitagawa, *Chem. Soc. Rev.* **40**, 696-753 (2011).
2. M. Sadeghi, G. Khanbabaei, A. Dehaghani, M. Sadeghi, M. Aravand, M. Akbarzade and S. Khatti, *J. Membrane Sci.* **322**, 423-428 (2008).
3. W. Bahloul, V. Bounor-Lagaré, L. David and P. Cassagnau, *J. Polym. Sci. Part B: Polym. Phys.* **48**, 1213-1222 (2010).
4. K. Wang, M. Choi, C. Koo, Y. Choi and I. Chung, *Polymer* **42**, 9819-9826 (2001).
5. L. J. Taylor, U.S. Patent No. 3,891,594 (1975).
6. P. Judeinstein and C. Sanchez, *J. Mater. Chem.* **6**, 511-525 (1996).
7. C. Xu, K. Ohno, V. Ladmiral and R. Composto, *Polymer* **49**, 3568-3577 (2008).
8. M. Rong, M. Zhang, Y. Zheng, H. Zeng, R. Walter and K. Frieddrich, *Polymer* **42**, 167-183 (2001).
9. X. Liua, Q. Wu, *Polymer* **42**, 10013-10019 (2001).
10. M. Oliveira, R. Nogueira and A. Machado, *React. Funct. Polym.* **72**, 703-712 (2012).
11. Y. Shieh, J. Liau and T. Chen, *J. Appl. Polym. Sci.* **81**, 186-196 (2001).
12. V. Bounor-Legaré, I. Ferreira, A. Verbois, P. Cassagnau and A. Michel, *Polymer* **43**, 6085-6092 (2002).
13. S. Patel, S. Malone, C. Cohen, J. Gilmor and H. Colby, *Macromolecules* **25**, 5241-5251 (1982).
14. C. F. Antunes, A. V. Machado and M. Duin, *Rubber Chem. Technol. J.* **82**, 492-505 (2009).